

Compton profile study of V_3Ge and Cr_3Ge

Y C SHARMA^{1,*}, V VYAS², V PURVIA², K B JOSHI³ and B K SHARMA²

¹Department of Physics, Swami Keshvanand Institute of Technology,
Jaipur 302 025, India

²Department of Physics, University of Rajasthan, Jaipur 302 004, India

³Department of Physics, University College of Science, M.L.S. University,
Udaipur 313 001, India

*Corresponding author. E-mail: yogeshchandra.sharma@gmail.com;
bkrish@sancharnet.in

Abstract. In this paper the results of a Compton profile study of two polycrystalline A15 compounds, namely, V_3Ge and Cr_3Ge , have been reported. The measurements have been performed using 59.54 keV γ -rays from an ^{241}Am source. The theoretical Compton profiles have been computed for both the compounds using *ab-initio* linear combination of atomic orbitals (LCAO) method employing CRYSTAL98. For both the A15 compounds, the isotropic experimental profiles are found to be in good overall agreement with the calculations. The comparison points out residual differences in V_3Ge whereas for Cr_3Ge the differences are within experimental error. The behaviour of valence electrons in the two iso-structural compounds has been examined on the scale of Fermi momentum. The valence electron distribution seems to be dominated by the metallic constituents rather than Ge and two compounds show covalent nature of bonding which is larger in V_3Ge compared to Cr_3Ge .

Keywords. A15 compounds; Compton profile; electronic structure; linear combination of atomic orbital method.

PACS Nos 71.15.Ap; 71.20.Ps; 74.70.Ad; 32.80.Cy

1. Introduction

A15-type compounds have been the subject of interest due to exotic electronic properties like optimum superconductivity and marginal structural stability [1]. Prior to the discovery of oxide superconductors, A15 compounds were known to display highest transition temperatures (T_c s) in the range of 18–23 K [2]. The structural instability and the temperature-dependent anomalies in the elastic constants were also realized to be due to exotic electronic structure. With the advent of high T_c superconductors, the interest on A15 compounds ceased and major thrust shifted to cuprates and related compounds with a view to understand the superconductivity and to discover the high T_c superconductors for promising technological applications. However, A15 compounds continued to be the subject of investigation due to other specific properties like structural anomalies, interplay of superconductivity

and structural phase transitions, temperature-dependent anomalies in elastic properties, phonon spectra, electrical resistivity, Knight shift, magnetic susceptibility etc. Consequently, structural, electronic, magnetic, elastic, vibrational and superconducting properties of these materials were widely studied through electronic structure calculations performed by several workers [3].

Most of the theoretical calculations have been attempted using APW [4–7], LMTO [8], LAPW [9] and the pseudopotential method [10] with a view to unravel electronic density of states, charge density, band structure and elastic anomalies. V_3Ge and Cr_3Ge are representative A15 compounds. Compared to other A15-type compounds, these two materials have received less attention. Although a number of LDA-based calculations have been performed for V_3Ge using APW, LMTO and LAPW methods, only a few theoretical studies are reported for Cr_3Ge due to the complexity involved in treating the valence electrons of chromium which shows unusual magnetic properties. Among experimental studies, the XPS and XES measurements have been reported on V_3Ge and some other A15 compounds [11]. X-ray diffraction [12] and 2D-ACAR measurements on A15 compounds have been reported by a number of workers [13]. Electron charge density analysis on different planes derived from the X-ray diffraction data has been demonstrated on V_3Ge [14]. The neutron and electron Raman scattering [15], de Haas-van Alphen measurements [16] and photoemission spectroscopy [17] have also been applied to study different A15 compounds. Due to the complexity involved in treating the Cr electrons, only a few theoretical studies have been performed for Cr_3Ge whereas a number of experimental studies have been reported to explore its physical and magnetic properties [18,19]. On the basis of K-edge and L-emission spectra and absorption edge, chemical bonding and charge transfer in a number of Cr–Ge systems including Cr_3Ge have also been discussed [20]. The chemical bonding and electronic structure of a number of Cr–Ge compounds were studied by XPS, X-ray and neutron diffraction techniques [21].

The inelastic scattering of X-rays from electrons at large momentum transfer, known as Compton scattering, is a unique probe to study the ground state electron momentum densities [22]. The technique is insensitive to crystal defects of the samples. The Compton profile, $J(p_z)$, is derived from the measured differential scattering cross-section. It is simply the projection of the electron momentum density $\rho(\mathbf{p})$ along the scattering vector (generally chosen as z -axis in the three-dimensional coordinate system). The double differential cross-section is related to the Compton profile as follows:

$$\frac{d^2\sigma}{d\Omega d\omega} \propto J(p_z) = \int_{-\infty}^{+\infty} \int_{-\infty}^{+\infty} \rho(\mathbf{p}) dp_x dp_y. \quad (1)$$

Also, the integral over the Compton profile is normalized to the number of electrons in the target, due to the normalization of the ground-state electron wave function $\psi(\mathbf{r})$.

Interestingly, on a reasonably fine energy scale, there are not many experimental possibilities to test a theoretically determined band structure, especially close to Fermi energy E_F . However, the states at E_F can be probed with a high degree of accuracy, and efforts have been made to map the Fermi surface for some A15 compounds by means of positron annihilation experiments [13] and de Haas-van Alphen

(dHvA) measurements [16]. Both these techniques as well as photoemission spectroscopy require high purity samples in identifying the electron states at E_F which are important to delineate the electron states responsible for the electronic properties and the fundamental physics underlying. In so far as the ground state electron momentum density and related quantities are concerned, to our knowledge, none of the A15 compounds have been studied. Thus, it is found worthwhile to perform Compton profile measurements and also to attempt the theoretical calculations for the two A15 compounds V₃Ge and Cr₃Ge. It would enable verification of the calculated bands around the Fermi energy and provide comparison of the nature of electronic states in the two compounds.

In this paper the theoretical and experimental Compton profile studies of the two A15 compounds, namely, V₃Ge and Cr₃Ge, are presented. The choice of polycrystalline samples was due to difficulty in getting the required size (12 mm dia. and 2 mm thickness) single crystals of these materials. Moreover, it enables comparison of relative nature of bonding in these compounds on valence-electron-density scale. To undertake Compton measurements, we have used our 5Ci ²⁴¹Am Compton spectrometer with a momentum resolution of 0.56 a.u. For the theoretical computations, LCAO calculations have been performed using CRYSTAL98 [23]. To compare the valence electron states in the two isostructural compounds, valence electron density (VED) analysis of the experimental and theoretical Compton profiles due to valence electrons is also performed.

Henceforth, all the quantities are given in atomic units (a.u.) where $e = m = \hbar = 1$ and $c = 137.036$ and the unit of length is equal to the Bohr radius. The SI equivalent of 1 a.u. of momentum is $1.99289 \times 10^{-24} \text{ kg m s}^{-1}$ which is, for example, close to the momentum of an electron at the Fermi surface in Al.

2. Measurements

The samples were prepared by the method reported in an earlier paper on V–Si compounds [24]. Samples of V₃Ge and Cr₃Ge were prepared at Uppsala, Sweden by arc melting the constituents (99.99% purity). The ingots were annealed in argon atmosphere. The X-ray diffraction confirmed their structure. The discs of required thickness were cut by diamond wafering saw from the annealed ingots. The V₃Ge sample was a disc of 15.6 mm diameter and 1.3 mm thickness whereas the sample of Cr₃Ge had a diameter of 16.3 mm and a thickness of 1.6 mm. The measurements were performed using the ²⁴¹Am radioisotope-based Compton spectrometer [25]. The scattered γ -rays were detected by HPGe detector (Canberra model GL0110P). The scattering angle was $165^\circ \pm 2.5^\circ$ leading to the overall momentum resolution of 0.56 a.u. The targets were housed in a vacuum chamber ($\sim 10^{-2}$ Torr). The spectra were recorded with a multichannel analyzer (MCA) with 4096 channels. The channel width was kept as ~ 20 eV, corresponding to 0.03 a.u. of momentum. The Compton scattering spectra were measured for around 25 h with total peak counts greater than 52,000 for V₃Ge and 50,000 for Cr₃Ge. The system was checked for stability by using a weak ²⁴¹Am source. To minimize the effect of escape peaks, the spectrum of the ²⁴¹Am calibration source was subtracted from the measured Compton spectra until

the elastic component disappeared. To correct for the background, measurement with sample holder was performed for 22 h and the scaled intensity was subtracted from the measured spectra. The signal-to-background ratio was found to be 450 : 1. The measured profile was then corrected for the effects of the detector response function, energy-dependent absorption and scattering cross-section [26]. The data reduction for the detector response function was restricted to stripping the low energy tail off the resolution function and smoothing the data, leaving a residual function for convoluting theory equivalent to a Gaussian of 0.56 a.u. width. After converting the profile to the momentum scale, a Monte Carlo simulation of the multiple scattering was performed. To account for the multiple scattering effects, we considered the history of approximately 1×10^7 photons. The profiles were then normalized to 44.56 electrons and 46.01 electrons for V_3Ge and Cr_3Ge , in the momentum range 0 to +7 a.u. at the interval of 0.1 a.u., being the area of free atom Compton profiles in the given range [27]. The 1s electrons of Ge were neglected for both the cases since they do not contribute to the experimental profile at the large momentum transfer for our experimental set-up.

3. Computational details

CRYSTAL98 program has been used to compute the theoretical Compton profiles in this study [23]. The code employs LCAO method under the HF and DFT methodologies. The crystalline orbitals used as basis for the wave function expansion were constructed from linear combination of atom centered Gaussian orbitals. An 86-4113G basis set was chosen for vanadium [28] and chromium [28] whereas 86-41G basis set was taken for germanium [28] to construct the LCAO basis for V_3Ge and Cr_3Ge . The exponents and contraction coefficients were further obtained by minimizing the total energy for the two compounds. The optimal exponents of the valence 5sp shell were obtained to get the minimum energy for the two compounds. To ensure convergence and achieve numerical accuracy, tight tolerance (10^{-6}) were given to evaluate Coulomb and exchange series, exchange overlap, Coulomb overlap, Coulomb penetration and the first exchange pseudo-overlap. For the second exchange, pseudo-overlap tolerance of 10^{-12} was considered at 84 k -points within the irreducible Brillouin zone corresponding to the shrinkage factor of 12 in Monkhorst net [29]. A dense Gilat net [30] of $12 \times 12 \times 12$ was chosen in reciprocal space. In general, 15 to 20 cycles were found sufficient to achieve convergence of the order of 10^{-6} Hartree per primitive cell. The unrestricted Hartree–Fock scheme [31] was adopted to determine the total energy for Cr_3Ge .

4. Results and discussion

The isotropic experimental Compton profiles of polycrystalline V_3Ge and Cr_3Ge are presented in tables 1 and 2 respectively for some selected values of p_z ranging from 0 to +7 a.u. Errors at a few points are also given. Also given here are the theoretical (unfolded) directional Compton profiles for both the materials along the principal crystallographic directions, namely, [1 0 0], [1 1 0], and [1 1 1] together with

Compton profile study of V₃Ge and Cr₃Ge

Table 1. Unconvoluted theoretical directional Compton profiles of V₃Ge along a few principal directions and the average Compton profile computed by CRYSTAL98. The last column shows isotropic experimental Compton profile together with the experimental errors at some points. All the profiles are in e/a.u. and are normalized to 44.56 electrons.

p_z (a.u.)	J_{100}	J_{110}	J_{111}	$J_{ave.}$	Expt.
0.0	20.806	20.649	21.125	20.791	21.969±0.056
0.1	20.781	20.587	20.948	20.712	21.902
0.2	20.666	20.370	20.494	20.477	21.649
0.3	20.411	20.007	19.944	20.125	21.210
0.4	19.949	19.541	19.347	19.642	20.600
0.5	19.321	19.090	18.752	19.076	19.833
0.6	18.540	18.621	18.167	18.419	18.937
0.7	17.666	18.052	17.642	17.707	17.949
0.8	16.674	17.224	17.054	16.876	16.899
1.0	14.337	14.723	15.069	14.678	14.774±0.045
1.2	11.811	11.870	12.110	11.985	12.821
1.4	9.707	9.620	9.601	9.678	11.087
1.6	8.143	8.042	8.005	8.049	9.713
1.8	6.905	6.834	6.811	6.820	8.469
2.0	5.918	5.873	5.825	5.855	7.495±0.032
3.0	3.338	3.338	3.337	3.337	4.319±0.023
4.0	2.358	2.359	2.359	2.359	2.838±0.018
5.0	2.082	2.082	2.082	2.082	1.995±0.015
6.0	1.562	1.562	1.562	1.562	1.489±0.013
7.0	1.183	1.183	1.183	1.183	1.085±0.011

the average Compton profiles. From the tables, it is visible that all the experimental values smoothly approach the theoretical values in the high momentum region, i.e. 3 to +7 a.u. The differences are negligible, as expected since in this region the contribution comes entirely due to core electrons.

For rigorous comparison, the convoluted theoretical and experimental isotropic Compton profiles are plotted in figures 1 and 2 for V₃Ge and Cr₃Ge, respectively. The theoretical results are folded with a Gaussian function of width 0.56 a.u. To examine the differences between experiment and the convoluted theoretical profiles, quantitatively on a fine scale, the difference ΔJ (Theo.–Expt.) for the two materials are presented in the lower panels. It is clear from the figures that the agreement between theory and experiment is very good. The differences of very small magnitude are, however, remaining as shown by the lower panels of the two figures. In the case of V₃Ge, the theory follows the experiment in the high momentum region, i.e. beyond 3.5 a.u. In the low momentum region, the experiment is higher than the theory up to 0.5 a.u. and afterwards becomes smaller than the theory. The maximum difference shown by the theory is at ~ 1 a.u. which is ~ 0.8 e/a.u. It amounts to only 1.7% of the total electrons whose distribution is under investigation in the V₃Ge pointing that the theory closely resembles the experiment in the entire range of momentum. In

Table 2. Unconvoluted theoretical directional Compton profiles for Cr₃Ge. The experimental isotropic Compton profile for Cr₃Ge is also listed in the last column with errors at some selected points. All the profiles are in e/a.u. and are normalized to 46.01 electrons.

p_z (a.u.)	J_{100}	J_{110}	J_{111}	$J_{ave.}$	Expt.
0.0	22.383	21.638	21.157	21.795	21.489±0.055
0.1	22.331	21.604	21.094	21.719	21.371
0.2	22.093	21.366	20.889	21.457	21.113
0.3	21.677	20.902	20.587	21.064	20.712
0.4	21.094	20.267	20.114	20.502	20.179
0.5	20.406	19.549	19.498	19.803	19.521
0.6	19.524	18.734	18.766	18.947	18.752
0.7	18.365	17.842	17.948	17.947	17.897
0.8	17.029	16.915	17.051	16.876	16.985
1.0	14.482	15.055	15.125	14.865	15.075±0.047
1.2	12.482	13.249	13.364	13.111	13.252
1.4	11.044	11.623	11.788	11.561	11.657
1.6	9.852	10.241	10.379	10.197	10.240
1.8	8.835	9.077	9.151	9.018	9.054
2.0	7.966	8.032	8.091	7.992	8.019±0.033
3.0	4.584	4.625	4.629	4.619	4.732±0.025
4.0	3.024	3.031	3.028	3.033	3.066±0.020
5.0	2.200	2.175	2.172	2.178	2.136±0.016
6.0	1.629	1.626	1.623	1.627	1.569±0.013
7.0	1.238	1.235	1.233	1.235	1.245±0.012

the case of Cr₃Ge, the lower panel shows even better agreement with the experiment. The maximum difference shown by the theory is at ~ 1.7 a.u. which is ~ 0.08 e/a.u. It amounts to less than 0.2% of the total electrons whose distribution is under consideration in Cr₃Ge. Specifically, for Cr₃Ge the differences in the entire range are within the experimental errors unlike V₃Ge. The agreement of this order clearly suggests that the basis sets considered to generate the Bloch orbitals and bands in Cr₃Ge are suitable for further usage and can be applied to explore other electronic properties of Cr₃Ge, which have not been studied rigorously. It may be important to note that HF scheme under the unrestricted approach [31] was applied for the Cr₃Ge where conventional HF is not applicable. To our knowledge no such comparison has been observed for compounds where UHF describes the electron states. Thus our study is encouraging and highlights possible application of the UHF scheme to study equation of state and related properties of materials where up and down spin electrons are treated separately to generate the Slater determinant. A marginal disagreement in the V₃Ge around the Fermi momentum may probably be due to the correlation effects.

To discuss the anisotropies in the calculated directional Compton profiles for the two materials, the convoluted anisotropies, i.e. $J_{111}-J_{100}$, $J_{110}-J_{100}$ and $J_{111}-J_{110}$ for V₃Ge are plotted in figure 3. The figure depicts that the overall trends of $J_{111}-J_{100}$ and $J_{110}-J_{100}$ are similar with a bias of about 0.12 a.u. The identical

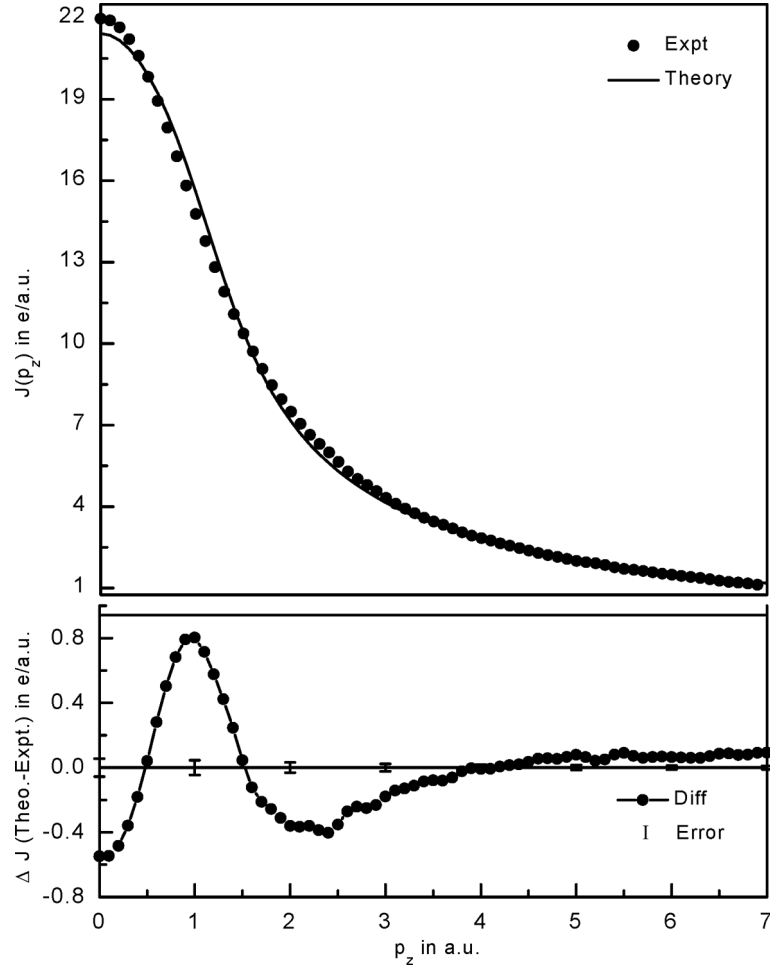


Figure 1. The upper panel shows total isotropic Compton profiles for V_3Ge . The solid circles represent the experiment whereas convoluted theory is represented by the solid line. The lower panel shows the difference (ΔJ) between the convoluted theory and the experiment.

trends in the anisotropies with respect to the $[100]$ direction are partially in agreement with the proposed Fermi surface dominated by the 3d bands of vanadium typically in V_3X ($X = Si, Sn$ and Ge) having hole-like structures along $[111]$ and $[110]$ directions and electron-like structures in the $[100]$ directions [5]. The larger number of holes along $[111]$ compared to $[110]$ direction are however not supported by our calculations. Our calculations show that the $J_{110}-J_{100}$ anisotropy is a bit larger than the $J_{111}-J_{100}$ in the momentum range ≤ 0.3 a.u., and thereafter the trend gets reversed. The different behaviour of the third anisotropy, i.e. $J_{111}-J_{110}$ in the low momentum region suggests that the charge occupancy contributing to the anisotropy is unlike the other two. It may be related to the Fermi surface of

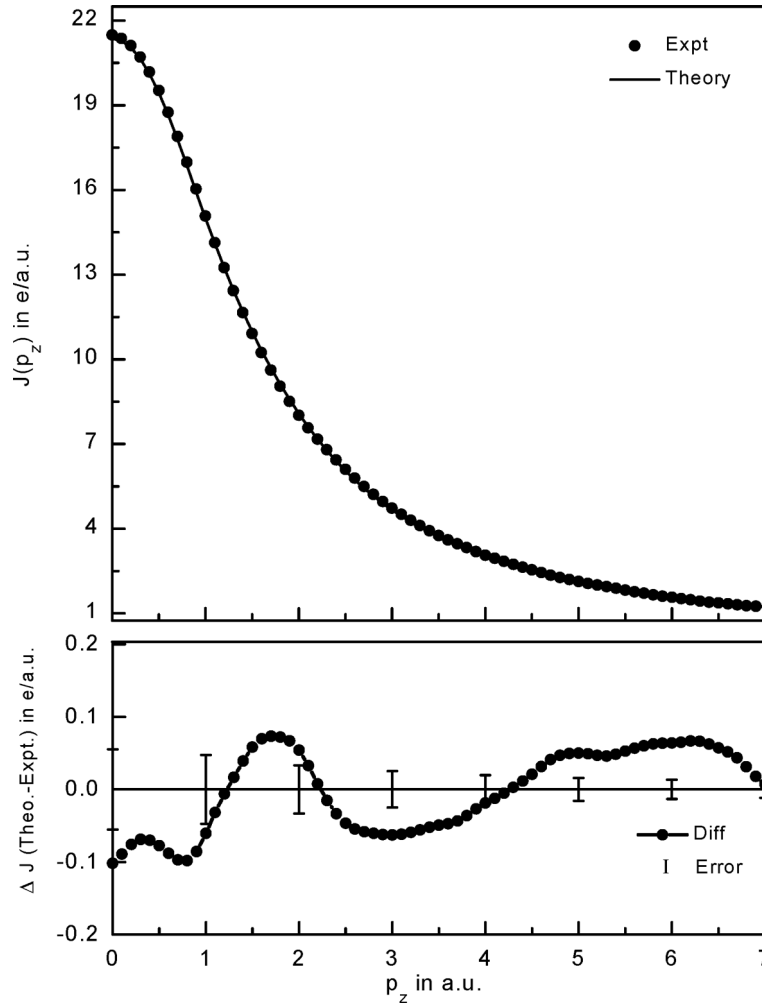


Figure 2. The upper panel shows total isotropic Compton profiles for Cr_3Ge . The solid circles represent the experiment whereas convoluted theory is represented by the solid line. The lower panel shows the difference (ΔJ) between the convoluted theory and the experiment.

V_3Ge . At the modest resolution offered by the present set-up, sharp features in the Fermi surface are not visible. It is also clear from the figure that the anisotropies are observable only up to 2.5 a.u. Beyond this, the isotropic contribution due to core electrons dominates in determining the momentum density and therefore anisotropy diminishes.

Unlike V_3Ge , Cr_3Ge has larger number of valence electrons and therefore the anisotropies in the directional Compton profiles of Cr_3Ge are expected to show enhanced features. To examine this, we have plotted three anisotropies, i.e. $J_{111}-J_{100}$, $J_{110}-J_{100}$ and $J_{111}-J_{110}$ for Cr_3Ge in figure 4. The anisotropies $J_{111}-J_{100}$

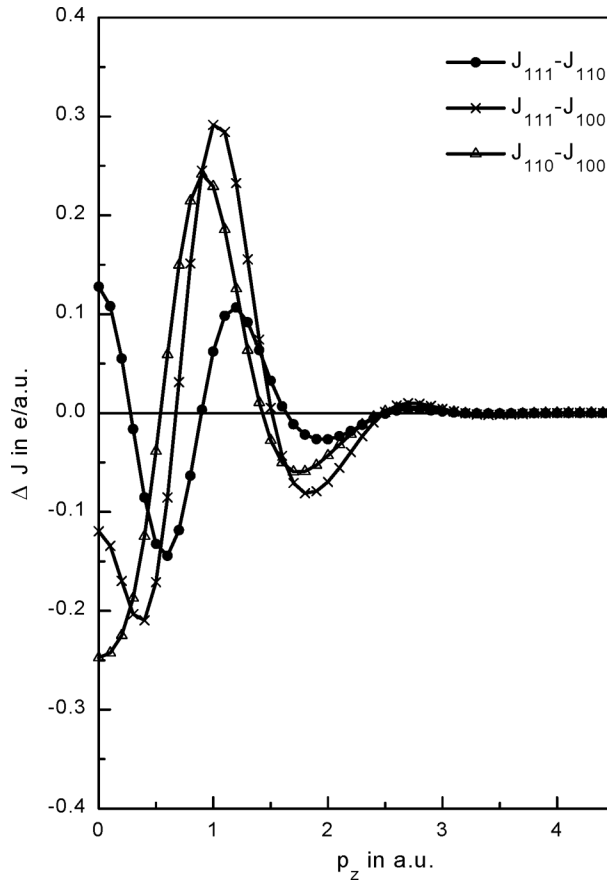


Figure 3. The convoluted directional anisotropies for V_3Ge obtained from the LCAO method.

and $J_{110}-J_{100}$ show extremes at $p_z = 1.5$ a.u. These extreme structures in the first anisotropy are almost twice the magnitude for V_3Ge . For the second anisotropy the corresponding magnitudes are ~ 2.5 times. As mentioned above, one possible reason could be the larger number of valence electrons (~ 11) in Cr_3Ge compared to V_3Ge (~ 9.5). The third anisotropy, however, differs substantially in the two cases. It may probably point that the anisotropies determined with respect to $[100]$ direction are more structure-dependent as compared to the $J_{111}-J_{110}$ which might involve reorganization of momentum density to a larger extent as this is different in the two materials.

In the absence of anisotropy measurements, the calculated directional Compton profiles are compared with theoretical average Compton profiles for V_3Ge and Cr_3Ge . In figure 5 the differences of folded theoretical directional Compton profiles and the calculated average Compton profile for V_3Ge are shown. The corresponding curves for Cr_3Ge are plotted in figure 6. Such comparison enables a study of relative occupancy along different planes of symmetry in momentum space. Figure 5 for

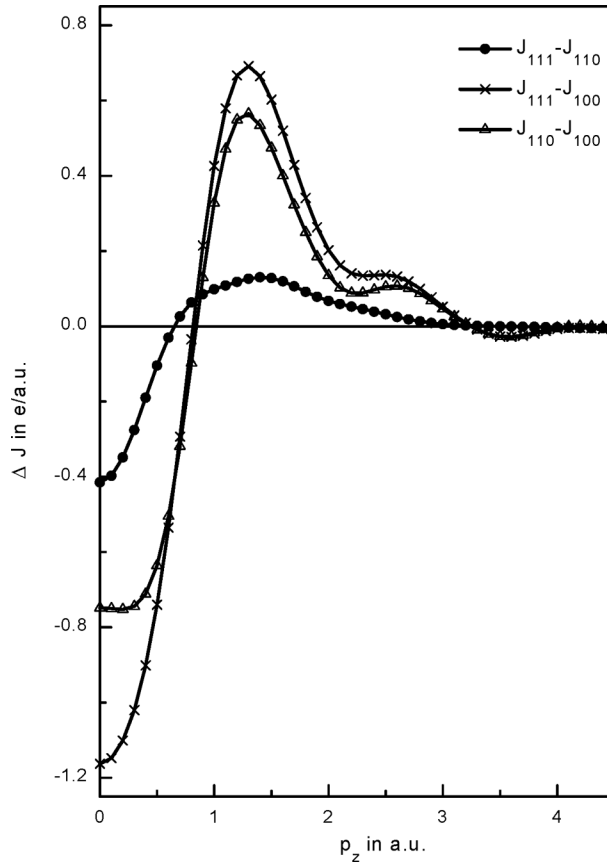


Figure 4. The convoluted directional anisotropies for Cr_3Ge obtained from the LCAO method.

V_3Ge depicts that the momentum density along $[110]$ is relatively lower and gradually increases along $[111]$ and $[100]$ directions. These may probably be due to the 3d vanadium bands. As suggested by Mattheiss [5], vanadium 3d bands split into two sub-bands along $\Gamma \rightarrow X$ and $\Gamma \rightarrow R$ directions but not along $\Gamma \rightarrow M$ leading to larger occupied states crossing along $[110]$ direction compared to the other two. The quantitative differences with our results may be due to the non-self-consistent nature of the APW method employed by Mattheiss [5] and the numerical accuracy of our calculations. Similar curves for Cr_3Ge are presented in figure 6. It points that the momentum density along $[100]$ is relatively larger than the $[110]$ and $[111]$ directions in the range $0.0 \leq p_z \leq 0.9$. One observes that in this range the states are least occupied along $[111]$ as compared to the other two directions. The trend gets reversed in $0.9 \leq p_z \leq 2.5$ a.u. Thus, the occupancies shown by the directional Compton profiles along $[100]$ direction for V_3Ge and Cr_3Ge relative to the average occupancy suggest that probably $[100]$ direction is more structure-dependent compared to the other two directions. One also observes that the relative occupancy shown along all the three directions in the two compounds are identical beyond

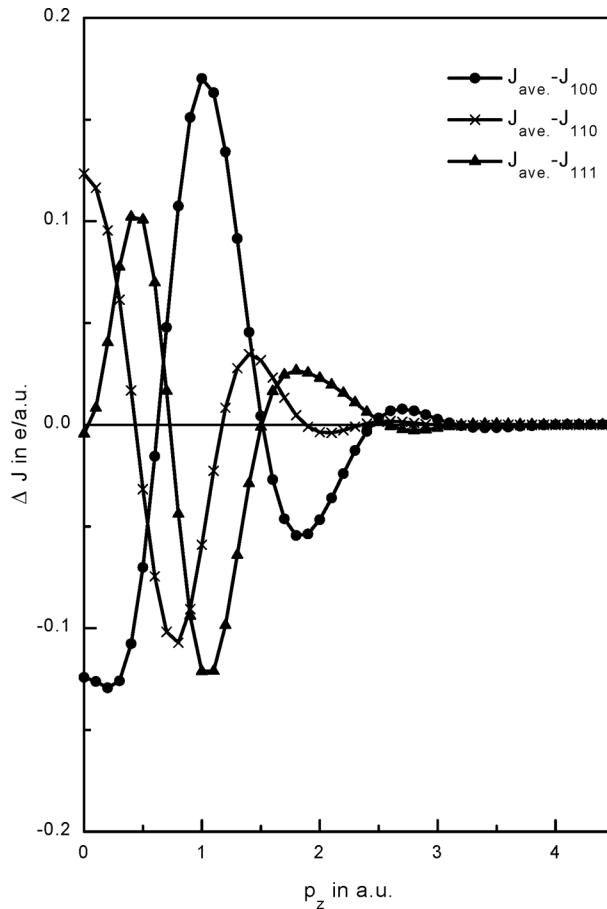


Figure 5. Difference between the convoluted average and directional Compton profiles for V_3Ge obtained from the LCAO method.

2.5 a.u. indicating the absence of direction-dependent features. The features appearing in the theoretical curve could be possibly due to the Fermi surface topology of Cr_3Ge . In order to explain the salient features, the highly resolved measurement of directional Compton profiles would be very useful.

In order to examine and compare the valence electron density distribution in the two iso-electronic compounds, the VED Compton profiles $[J(p_z) \times p_F]$ on p_z/p_F scale have been deduced. The valence electron density (VED) profiles are plotted on the scale of p_F in figures 7a and 7b with a view to examine the nature of bonding which to a first approximation will be identical for compounds with identical bonding. In the two compounds considered here valence contribution due to Ge may be identical and so the overall shape is presumably influenced by the metallic constituents. Despite having larger number of valence electrons in Cr, the VED profile for V_3Ge is larger up to 1.1 a.u. indicating more metallic behaviour in V_3Ge than in Cr_3Ge . From the VED plots shown in figure 7a, it is observed that the $J(0)$ values for V_3Ge

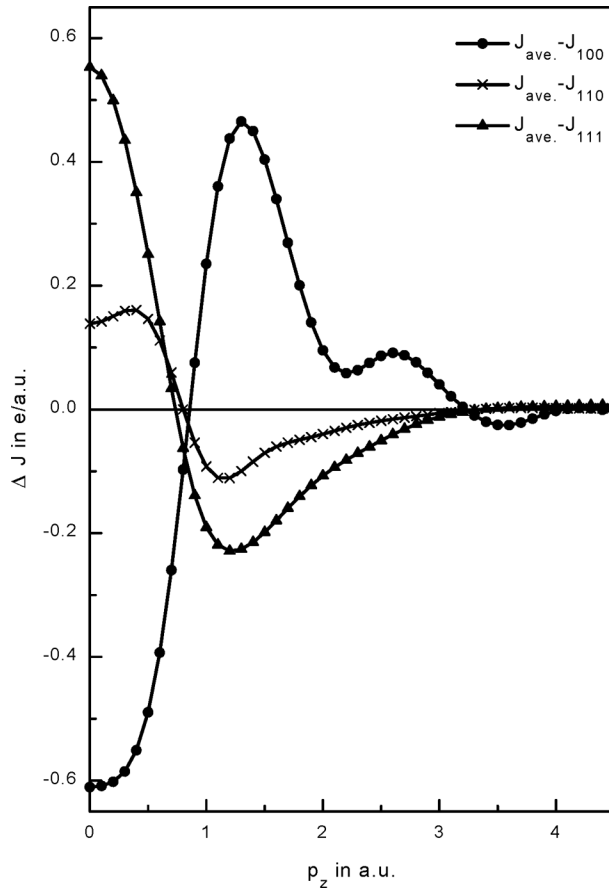


Figure 6. Difference between the convoluted average and directional Compton profiles for Cr_3Ge obtained from the LCAO method.

is about 15% larger than that for Cr_3Ge but the profile of Cr_3Ge has a larger tail. The same trend is observed in the theoretical VED profiles shown in figure 7b. As sharpness may be attributed to the localization of charge in real space leading to covalent bonding [32], larger (15%) value of $J(0)$ for V_3Ge as compared to Cr_3Ge clearly points larger covalent character of bonding in this compound. The covalent character predicted by both the curves for V_3Ge is in agreement with the findings of Klein and co-workers [6] who predicted strong covalent bond between V and Ge in addition to the strong V–V bonds. Similar conclusions have been reported for V_3Si and Cr_3Si which show larger build-up of charges between vanadium atoms than the Cr atoms on the basis of electron charge density maps [33]. To examine the directional nature of bonding more critically in these compounds, anisotropy measurements are required.

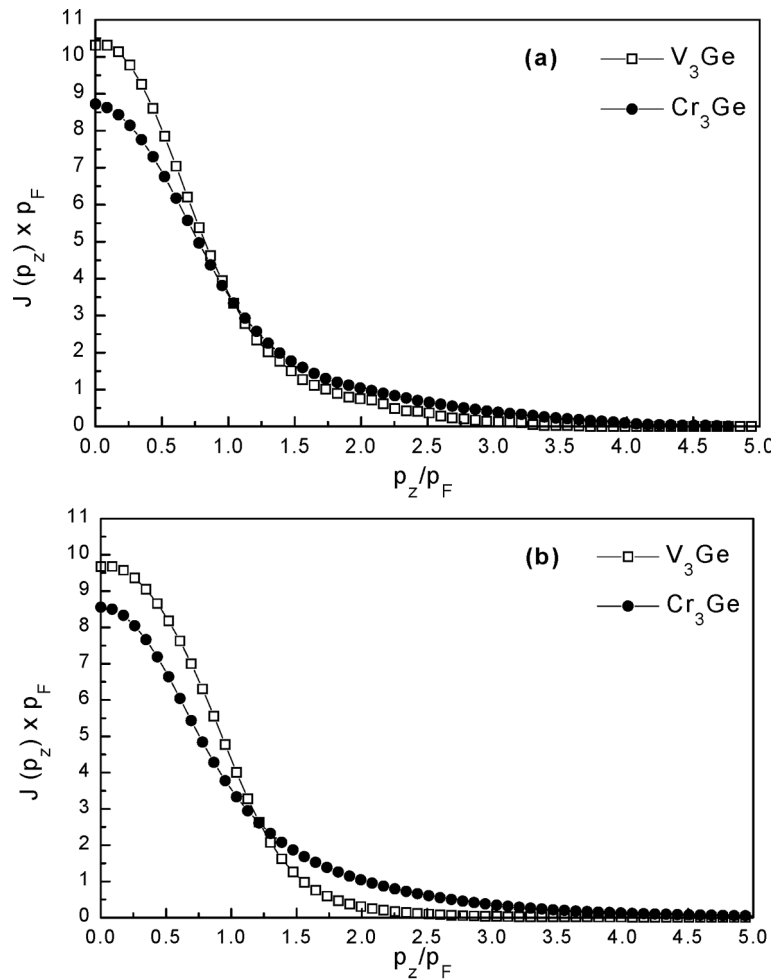


Figure 7. The equal-valence-electron-density profiles deduced from (a) experiment and (b) convolved theoretical Compton profiles for V_3Ge and Cr_3Ge .

5. Conclusions

The measured isotropic Compton profiles of A15 compounds V_3Ge and Cr_3Ge are compared with corresponding isotropic theoretical profiles computed using CRYSTAL98. The theory is in good overall agreement with the measurement for V_3Ge . The experimental data of Cr_3Ge are in excellent agreement with theory when the valence electrons are treated differently under the UHF scheme indicating a fundamental difference in the electronic states of the vanadium germanide and chromium germanide. Despite showing good overall agreement, residual differences between theory and experiment for V_3Ge remain which may probably be due to inadequate correlation corrections. The valence-electron-density profiles of the two A15

compounds show that the metallic constituents dominate the momentum density of valence electrons in V_3Ge and Cr_3Ge . The VED profiles also predict that the bonding in V_3Ge is covalent and covalency is larger than Cr_3Ge . The calculated anisotropies in V_3Ge are in reasonable agreement with the model Fermi surface and the reported APW band structure. It would be interesting to perform directional Compton profile measurements at high resolution and then comparison with our calculation of both the compounds would be worthwhile to delineate the Fermi surface calipers.

Acknowledgements

The financial support through projects SR/S2/M-45/1999 and SR/S2/CMP-15/2004 by the DST, New Delhi is gratefully acknowledged.

References

- [1] C P Poole Jr. (ed.), *Handbook of superconductivity* (Elsevier, New Delhi, 2006)
- [2] G F Hardy and J D Hulm, *Phys. Rev.* **87**, 884 (1953); *Phys. Rev.* **93**, 1004 (1954)
B T Matthias, T H Geballe, S Geller and E Corenzwit, *Phys. Rev.* **95**, 1435 (1954)
- [3] J Muller, *Rep. Prog. Phys.* **43**, 641 (1980)
- [4] L F Mattheiss, *Phys. Rev.* **138**, A112 (1965)
- [5] L F Mattheiss, *Phys. Rev.* **B12**, 2161 (1975)
- [6] B M Klein, L L Boyer, D A Papaconstantopoulos and L F Mattheiss, *Phys. Rev.* **B18**, 6411 (1978)
- [7] A T van Kessel, H W Myron and F M Mueller, *Phys. Rev. Lett.* **41**, 181 (1978); *Phys. Rev. Lett.* **41**, 520 (1978)
- [8] G Arbmán and T Jarlborg, *Solid State Commun.* **26**, 857 (1978)
T Jarlborg, A Junod and M Peter, *Phys. Rev.* **B27**, 1558 (1983)
P Ravindran and R Asokamani, *Phys. Rev.* **B50**, 668 (1994)
- [9] Z W Lu and B M Klein, *Phys. Rev. Lett.* **79**, 1361 (1997)
- [10] W E Pickett, K M Ho and M L Cohen, *Phys. Rev.* **B19**, 1734 (1979)
- [11] T Jarlborg and P O Nilsson, *J. Phys.* **C12**, 265 (1979)
- [12] P Chaddah and R O Simmons, *Phys. Rev.* **B27**, 119 (1983)
- [13] S Samoilov, M Weger, I Nowik, I B Goldberg and J Ashkenazi, *J. Phys.* **F11**, 1281 (1981) and references therein
- [14] J-L Staudenmann, B DeFacio and C Stassis, *Phys. Rev.* **B27**, 4186 (1983)
- [15] S B Dierker, M V Klein, G W Webb and Z Fisk, *Phys. Rev. Lett.* **50**, 853 (1983)
R Hackl, R Kaiser and S Schick Tanz, *J. Phys.: Condens. Matter* **16**, 1792 (1983)
R Hackl, R Kaiser and W Gläser, *Physica (Amsterdam)* **C162**, 431 (1989)
- [16] F M Mueller, D H Lowndes, Y K Chang, A J Arko and R S List, *Phys. Rev. Lett.* **68**, 3928 (1992)
T J B Janssen, C Haworth, S M Hayden, P Meeson, M Springford and A Wasserman, *Phys. Rev.* **B57**, 11698 (1998)
- [17] F Reinert, G Nicolay, B Eltner, D Ehm, S Schmidt, S Hüfner, U Probst and E Bucher, *Phys. Rev. Lett.* **85**, 3930 (2000)
- [18] S D Margolin and I G Fakidov, *Fiz. Met. Metalloved.* **9**, 823 (1960)

Compton profile study of V₃Ge and Cr₃Ge

- V L Zagryazhskii, P V Gel'd and A K Stol's, *Izv. Vyssh. Ucheb. Zaved. Fiz.* **11**, 46 (1968)
- [19] I G Fakidov and N P Grazhdankina, *Fiz. Met. Metalloved.* **6**, 67 (1958)
B Rawal and K P Gupta, *J. Less-Common Met.* **27**, 65 (1972)
- [20] I N Frantsevich, E A Zhurakovskii and V V Shvaiko, *Ukr. Fiz. Zh.* **21**, 1339 (1976)
- [21] M Kolenda, J Leciejewicz and A Szytula, *Phys. Status Solidi* **B57**, K107 (1973)
M Kolenda, J Stoch and A Szytula, *J. Magn. Magn. Mater.* **20**, 99 (1980)
- [22] M J Cooper, *Rep. Prog. Phys.* **48**, 415 (1985) and references therein
Also M J Cooper, P E Mijnarends, N Shiotani, N Sakai and A Bansil, *X-ray Compton scattering* (Oxford University Press, New York, 2004)
- [23] V R Saunders, R Dovesi, C Roetti, M Causà, N M Harrison, R Orlando and C M Zicovich-Wilson, *CRYSTAL98 User's manual* (University of Torino, 1998)
- [24] B K Sharma, S Manninen, T Paakkari, M W Richardson and S Rundqvist, *Philos. Mag.* **B49**, 363 (1984)
- [25] B K Sharma, A Gupta, H Singh, S Perkkio, A Kshirsagar and D G Kanhere, *Phys. Rev.* **B37**, 6821 (1988)
- [26] D N Timms, *Compton scattering studies of spin and momentum densities*, Ph.D. Thesis (University of Warwick, England, 1989) unpublished
- [27] F Biggs, L B Mendelsohn and J B Mann, *At. Data Nucl. Data Tables* **16**, 201 (1975)
- [28] <http://www.tcm.phys.cam.ac.uk/>
- [29] H J Monkhorst and J D Pack, *Phys. Rev.* **B13**, 5188 (1976)
- [30] G Gilat and J L Raubenheimer, *Phys. Rev.* **144**, 390 (1966)
- [31] C Pisani, R Dovesi and C Roetti, *Hartree-Fock ab-initio treatment of crystalline systems* (Springer-Verlag, Heidelberg, 1988) vol. 48
- [32] K B Joshi, R Jain, R K Pandya, B L Ahuja and B K Sharma, *J. Chem. Phys.* **111**, 163 (1999)
- [33] J-L Staudenmann, B DeFacio, L R Testardi, S A Werner, R Flükiger and J Muller, *Phys. Rev.* **B24**, 6446 (1981)